Mechanistic Insights into Human Antimicrobial Peptide-Induced Activation of a Broadly Conserved Bacterial Signaling System

Samuel A. Adeleye[1], Abraham F. Mechesso[2], Arpita Mukherjee[1], Guangshun Wang*[,2], Srujana S. Yadavalli[1]*

[1]Waksman Institute of Microbiology and Department of Genetics, Rutgers University, Piscataway, New Jersey 08854 USA

[2]Department of Pathology and Microbiology, College of Medicine, University of Nebraska Medical Center, Omaha, Nebraska 68198 USA

*Corresponding authors: sam.yadavalli@rutgers.edu, gwang@unmc.edu

Short title: Peptide-induced activation of a bacterial signaling system

Classification: Biological Sciences, Microbiology

Keywords: Bacteria, antimicrobial peptides, two-component signaling systems, stress response, cell elongation, reporter gene assays

Abstract

Antimicrobial peptides (AMPs) represent a promising class of therapeutics against bacterial pathogens. While their direct bactericidal mechanisms are well-characterized, how bacteria sense and respond to these peptides at sublethal concentrations remains poorly understood. Here, we investigate the activation of the *Escherichia coli* PhoQ-PhoP signaling system by the human antimicrobial peptide LL-37 and its derivatives (KR-12 and RI-10). We demonstrate that these peptides exhibit variable antimicrobial potency but surprisingly similar abilities to activate the PhoQ-PhoP pathway, indicating that signaling function is separable from bactericidal activity. Notably, sublethal concentrations of these peptides induce significant cell elongation, a phenotype dependent on PhoQ and mediated by the upregulation of QueE, which interferes with bacterial cell division. Contrary to the previous model suggesting peptides activate PhoQ passively by displacing its inhibitor MgrB, we observed enhanced cell elongation in *ΔmgrB* strains across all tested peptides, including RI-10, lacking antibacterial activity. Our findings suggest peptides actively stimulate PhoQ through a mechanism independent of MgrB dissociation, providing a more refined understanding of the peptide signaling through the PhoQ-PhoP system. These insights into bacterial adaptation mechanisms against host-derived peptides may guide the development of peptide therapeutics with enhanced efficacy against drug-resistant pathogens.

Significance statement

Antimicrobial peptides (AMPs) are promising alternatives to conventional antibiotics, yet how bacteria detect and respond to these host defense molecules remains poorly understood. This study investigates the interaction between bacterial sensing systems and AMPs at the genetic and molecular levels. Unlike other eukaryotes with multiple cathelicidin peptides, humans have only one cathelicidin that produces various active fragments through processing. Rather than creating multiple detectors, *E. coli* deploys an elegant solution, the PhoQ-PhoP signaling system that recognizes the conserved antimicrobial region shared by all LL-37 fragments. We demonstrate that peptides directly stimulate PhoQ independent of their bactericidal activity, even in the absence of inhibitor MgrB, inducing cell elongation. These insights may inform the development of effective peptide-based therapeutics against drug-resistant pathogens.

62 ## Introduction

63 When exposed to specific cationic antimicrobial peptides (AMPs) at sublethal concentrations,
64 *Escherichia coli* activates the PhoQ/PhoP signal transduction pathway—a conserved two-
65 component system crucial for stress adaptation in Gram-negative bacteria (1, 2). The
66 PhoQ/PhoP signaling system is also an important pathway for adaptation and survival in
67 conditions such as low Mg^{2+}, mildly acidic pH, and hyperosmolarity in *E. coli* and closely related
68 enterobacteria (3, 4). Activated PhoQ-PhoP regulate numerous genes, including those
69 responsible for remodeling the outer membrane, activation of efflux pumps, and proteolytic
70 degradation of the peptides that help bacteria resist cationic AMPs (5–8). Strong activation of
71 the PhoQ-PhoP system is observed when cells are treated with a human platelet-derived AMP
72 (C18G), causing the upregulation of QueE, an enzyme primarily known for its role in the
73 queuosine biosynthetic pathway that modifies specific tRNAs (2). Remarkably, elevated QueE
74 levels lead to the accumulation of this protein at the bacterial division septum, where it interacts
75 with the cell division machinery. This interaction disrupts normal septation processes
76 downstream of Z-ring formation, resulting in inhibited cell division and the development of
77 filamentous bacterial morphology. This mechanism represents a sophisticated bacterial stress
78 response that temporarily halts proliferation when facing host antimicrobial challenges.
79
80 Human cathelicidin, LL-37, is one of the best-studied AMPs (9–11) with a broad spectrum of
81 activity against bacteria, fungi, parasites, viruses, and cancer cells (11–15). LL-37 is known to
82 activate the PhoQ-PhoP system and exert its antimicrobial action primarily by interacting with
83 bacterial membranes, inserting itself into the lipid bilayer, and leading to membrane
84 destabilization and the formation of pores (1, 16–18). This disruption results in the loss of
85 membrane integrity, causing leakage of cellular contents and ultimately leading to bacterial cell
86 death. LL-37's efficacy against pathogens is influenced by the composition of the growth

87 medium, particularly the presence of high salt concentrations and divalent cations (19). In our
88 current understanding, cationic antimicrobial peptides interact with the acidic patch in the
89 periplasmic sensing domain of PhoQ, displacing divalent cations (particularly Mg^{2+}) that
90 normally repress PhoQ activity, leading to PhoQ autophosphorylation and subsequent
91 phosphorylation of PhoP (1). Besides peptides and other signals, a 47 amino acid long small
92 membrane protein called MgrB interacts with and inhibits PhoQ by affecting its kinase activity
93 (20, 21). Specific residues in the transmembrane and periplasmic regions of MgrB are important
94 for the interaction with PhoQ (22). It is proposed that the sensing of AMPs by PhoQ at
95 physiological concentrations of magnesium is dependent on MgrB (23). A conformational
96 change in PhoQ upon AMP binding is thought to disrupt the PhoQ-MgrB complex, resulting in
97 PhoQ activation via derepression. This model suggests that AMPs play an inert role in
98 stimulating PhoQ.
99
100 Human cathelicidin LL-37 contains 37 amino acids and starts with a pair of leucine residues.
101 Triple-resonance NMR structural studies established that the C-terminal tail of LL-37 (residues
102 33-37) is disordered and not required for membrane-targeting mediated antimicrobial activity
103 (24). This led to the use of several derivatives of the LL-37 peptide from the central region for
104 therapeutic development (11, 24, 25). KR-12 is a 12-amino acid-long, truncated peptide derived
105 from human LL-37, which is toxic to bacteria but not human cells (24). It has been widely utilized
106 in peptide engineering (26). To effectively develop AMPs as novel peptide therapeutics, it is
107 imperative to study the bacterial response to these peptides, including the biochemical and
108 regulatory pathways that underlie this process. While there has been tremendous progress in
109 establishing the direct antimicrobial action of AMPs such as LL-37 against bacteria (27), much
110 less is known about the phenotypic changes elicited by these peptides at sub-lethal doses and
111 how their length and sequence contribute to bacterial response. In addition, it is unclear if AMPs
112 have a direct and active role in stimulating PhoQ.

113 To gain deeper insights into the stress response mechanism to AMPs in *E. coli*, we utilized LL-
114 37, its shortest anti-*E. coli* peptide KR-12, and an even shorter non-antibacterial peptide RI-10,
115 resulting from the truncation of the N-terminal lysine and C-terminal arginine of KR-12. In
116 particular, we first examined the antibacterial activity of LL-37 and its smaller fragments, KR-12
117 and RI-10, using different *E. coli* strains under physiologically relevant conditions. We
118 determined the killing kinetics and characterized the peptides using membrane permeabilization
119 and depolarization assays. Next, we investigated whether LL-37 and its fragments, at
120 concentrations below MIC, are effective in activating the PhoQ/PhoP signaling system by
121 analyzing both the changes in cell morphology and PhoP-dependent transcriptional reporter
122 activity as readouts. Finally, based on our analysis of cells lacking the PhoQ inhibitor, MgrB, we
123 propose a model of how peptides like LL-37 and its derivatives may interact with bacterial
124 histidine kinase and affect bacterial physiology. Our study sheds light on the molecular
125 mechanism of bacterial detection of biologically relevant peptide LL-37, which is known to play a
126 key role in human health via both antimicrobial and immune regulatory roles (9-12,27). Our
127 results reveal that the bacterial PhoQ-PhoP two-component system detects a variety of LL-37
128 antimicrobial fragments in a specific manner by recognizing the consensus core antimicrobial
129 region.
130

131 ## Results

132 **Antibacterial activity of LL-37 and its derivatives against *E. coli*.**

133 To better delineate the antibacterial activity of LL-37, KR-12, and RI-10 against *E. coli*, we
134 compared both their minimum inhibitory concentration (MIC) and minimum bactericidal
135 concentration (MBC) against four *E. coli* strains (MG1655, E423-17, E416-17, and 25922,
136 Tables 1, S1, S2) under three different media conditions: Mueller Hinton Broth (MHB), tryptic
137 soy broth (TSB), or supplemented minimal A medium (MinA). Gentamicin was included as a

138 non-peptide antibiotic control. LL-37 exhibited the highest potency with MIC values between 2
139 and 8 μM, depending on the media used (Table 1). Interestingly, the KR-12 peptide, which is
140 shorter than LL-37 by 25 amino acids, is also active against the *E. coli* isolates tested. The MIC
141 and MBC values for KR-12 are similar or 2-4 fold higher than those obtained for LL-37. The
142 values obtained in minimal medium were in a similar range as those obtained in other media,
143 especially for *E. coli* K-12 MG1655 strain (Tables 1, S1). The shortest LL-37 variant, RI-10, did
144 not show antibacterial activity against any of the isolates tested here across different media
145 conditions, or after dilution of MHB to 10%. From here on, for characterization of the
146 antibacterial and physiological effects of these peptides, we used the *E. coli* MG1655 strain
147 grown in the supplemented minimal medium. Next, we investigated the time-dependent killing
148 kinetics of LL-37, KR-12, and RI-10 to further substantiate their bactericidal properties using a
149 concentration corresponding to 2x MIC values (Figure S1). LL-37 (2× MIC) completely
150 eradicated the exponential phase of *E. coli* K-12 MG1655 in 1 hour, while KR-12 caused about a
151 4-log fold reduction in 2 hours. As expected, RI-10 displayed no activity at the concentration
152 tested. Together, these results show that full-length LL-37 and KR-12 exhibit antibacterial
153 properties against *E. coli* but not RI-10.
154
155 **LL-37 and KR-12, but not RI-10, disrupt bacterial membranes.**
156 Given that LL-37 targets bacterial membranes, we wondered if the shorter peptide variants, KR-
157 12 and RI-10, may retain and exhibit activity against *E. coli* membranes. To assess membrane
158 disruption, we conducted membrane permeabilization and depolarization experiments. We
159 analyzed membrane permeability by the uptake of a membrane-impermeable red dye,
160 propidium iodide (PI), either in the presence of a peptide, 0.1% Triton-X (positive control) or
161 PBS (untreated). Treatment with either LL-37 or KR-12 led to an increase in membrane
162 permeability in a dose-dependent manner, although LL-37 was more effective (Figure 1A-C). To
163 assay membrane depolarization, we used $DiBAC_4(3)$, a probe for membrane potential, whose

164 fluorescence increases upon entering depolarized cells. As expected, LL-37 depolarized
165 membranes well with increasing concentration of the peptide (Figure 1D-F). Similarly, KR-12
166 also caused membrane depolarization but to a lower extent relative to LL-37. Consistent with
167 the data from MIC assay and killing kinetics, RI-10 did not have a discernible effect on
168 membrane permeability and depolarization. Together, these results suggest that KR-12, like LL-
169 37, targets the bacterial membrane as its mode of action.
170
171 **Sub-MIC levels of LL-37 and KR-12 activate the PhoQ/PhoP signaling system and cause**
172 **cell elongation.**
173 Cationic antimicrobial peptides, LL-37 and C18G activate the PhoQP pathway in *E. coli* and
174 related bacteria (1, 2). In addition, *E. coli* cells elongate upon exposure to a sub-lethal dose of
175 C18G, leading to filamentous growth (2). This filamentation is associated with conditions that
176 strongly activate PhoQ/PhoP. We asked if the truncated LL-37 derivatives retain the ability to
177 activate the PhoQP system. We used a promoter-reporter strain containing P_{mgrB}-*yfp* to measure
178 the transcriptional activity of the *mgrB* gene, whose expression is PhoQP-dependent. In parallel,
179 we observed the cells by phase contrast microscopy to test if the peptides induce any changes
180 in *E. coli* cell morphology. Our analysis revealed that there is a 3 to 3.5-fold increase in PhoQP-
181 regulated transcriptional activity when cells are treated with a sub-MIC dose of LL-37 at 1.25 μM
182 and KR-12 at 5 μM (Figure 2A). RI-10 showed weak activation of ~1.7-fold higher than the
183 untreated control. As the amino acid sequence of RI-10 (i.e., residues 19-28 of LL-37) is
184 included in both KR-12 (residues 18-29) and LL-37, we also asked how a different LL-37
185 segment, KE-10 (residues 10-19), with a minimal sequence overlap with KR-12 and RI-10
186 (Table S2), behaves. Like RI-10, KE-10 showed no antibacterial activity against *E. coli* (MIC >
187 64 μM in Table 1). In contrast to RI-10, the KE-10 peptide showed negligible activation of the
188 PhoQP system based on the transcription activity measurement of the *mgrB* gene, implying that
189 there is a requirement for a particular peptide sequence for this activation. Although LL-37 was

190 long known to activate the PhoQP system, its impact on *E. coli* cell morphology, especially at
191 concentrations below the MIC, has not been studied previously. Upon observation by phase
192 contrast microscopy, both LL-37 and KR-12-treated cells displayed elongation with
193 heterogeneous cell lengths (Figure 2B). The average cell lengths increased by ~1.5-fold for cells
194 exposed to LL-37 and KR-12 when compared to the control cells (Figure 2C). However, both RI-
195 10 and KE-10 treated cells did not show a significant change in cell length (Figure 2B-C).
196 Together, these data elucidate that LL-37, KR-12, and RI-10 are functional in stimulating the
197 PhoQP pathway and eliciting a physiological response, but not KE-10. However, only full-length
198 LL-37 and its minimal antibacterial peptide KR-12 are strong enough to cause morphological
199 changes similar to what was observed for the C18G peptide previously (2) , whereas two
200 shorter LL-37 segments (RI-10 and KE-10), which lost antibacterial activity, were unable to.
201
202 **Cell elongation caused by sub-MIC levels of peptides is dependent on PhoQ and QueE.**
203 To gain additional insight into the cell elongation caused by peptides, we examined the
204 morphology of the cells upon deletion of *phoQ*. As expected, Δ*phoQ* cells did not elongate when
205 treated with LL-37 and KR-12 (Figure 3A). There was no increase in PhoQP-dependent
206 transcriptional activity of P_{mgrB}, even in the presence of LL-37 and KR-12 in Δ*phoQ* cells (Figure
207 3B), and the average cell lengths were similar relative to the no-peptide control (Figure 3C),
208 confirming that the cell elongation phenotype associated with these AMPs is dependent on
209 PhoQ activation. In previous work, sub-MIC levels of C18G are shown to cause filamentation in
210 wild-type *E. coli* cells, which is mediated by increased expression of a PhoP-dependent gene
211 called *queE*, encoding a protein with dual activities in the inhibition of cell division and the
212 synthesis of queuosine tRNA modification (2, 28). We asked if the morphological phenotype
213 observed here for cells exposed to LL-37 and KR-12 is also mediated by QueE or through an
214 independent mechanism. Using a *queE* deletion strain, we carried out microscopy and
215 measured cell lengths and transcriptional reporter activity. Δ*queE* suppressed the elongation

216 phenotype observed when cells were treated with either LL-37 or KR-12 (Figures 3A, 2B). It is
217 worth noting that Δ*queE* cells grown in the presence of these peptides still display an increase in
218 PhoQP-regulated transcriptional reporter activity similar to the wild-type cells (Figures 3D, 2A).
219 Consistently, Δ*queE* cells exposed to peptides did not show a difference in the average cell
220 length relative to the controls (no peptide, KE-10, Figure 3E). Overall, filamentation and
221 heterogeneity in cell size observed upon treatment with LL-37 and KR-12 peptides are both
222 PhoQ- and QueE-dependent.
223
224 **Deletion of PhoQ inhibitor, MgrB, increases cell responsiveness to LL-37 and its**
225 **derivatives.**
226 *E. coli* cells, carrying an *mgrB* deletion, show an overall, robust increase in PhoQP-controlled
227 gene expression (20). These cells experience higher stimulation of PhoQ under magnesium-
228 limiting conditions, similar to the strong activation of this system observed in wild-type cells
229 grown in the presence of C18G at intermediate magnesium concentrations (2). Consequently,
230 Δ*mgrB* cells grow as long filaments, and this phenotype is dependent on upregulation of QueE
231 expression by PhoQ/PhoP (2). It is proposed that MgrB mediates the sensing of cationic AMPs
232 by PhoQ at intermediate concentrations of magnesium, therefore, LL-37, KR-12, and RI-10 may
233 activate PhoQ only when MgrB is present. In this case, we expect Δ*mgrB* cells to show no
234 significant change in either the PhoP-dependent transcriptional reporter activity or cell
235 morphology when treated with peptides vs. no treatment. We examined how LL-37 and its
236 derivatives influence the activity of the PhoQP system and cell lengths in a Δ*mgrB* strain. As
237 expected, in the absence of peptides, Δ*mgrB* cells showed an increase in P_{mgrB} transcription
238 relative to the wild-type cells under the same growth conditions (Figures 4A-B). When the AMPs
239 were added to Δ*mgrB* cells, there was a modest increase of ~1.4-fold in the PhoQP-regulated
240 transcriptional reporter activity for LL-37, as observed previously using the same media
241 conditions carrying 0.1 mM Mg^{2+} (Figure 4A) (20). The addition of peptides KR-12, RI-10, and

242 KE-10 did not lead to a substantial increase in reporter activity, suggesting that PhoP-mediated
243 transcription is not sensitive in response to the two peptides in cells lacking MgrB. This result is
244 consistent with a previous study where Δ*mgrB* cells did not show an increase in PhoP-regulated
245 transcription in the presence of another AMP, C18G (23).
246 To investigate this further, we analyzed the morphology of Δ*mgrB* cells in the presence of
247 peptides, wherein cell elongation is PhoQ-dependent and a direct function of strong PhoQP
248 activation. As expected, we noticed filamentation in Δ*mgrB* cells treated with LL-37 and KR-12,
249 but only short, typical cells in the KE-10-treated or no-peptide control cells, under this growth
250 condition with 0.1 mM Mg^{2+} (Figure 4C). It was intriguing, however, to see that RI-10-treated
251 Δ*mgrB* cells also displayed elongation, suggesting that RI-10 may interact more effectively with
252 PhoQ to activate it, in the absence of MgrB. In other words, loss of the inhibitor MgrB appears to
253 unmask the effect of RI-10 peptide on PhoQ stimulation, resulting in an evident cell elongation
254 phenotype. Interestingly, cell size quantification revealed greater heterogeneity and higher
255 average cell lengths across all three peptides for Δ*mgrB* of 6-8 μm (Figure 4D). The mean cell
256 lengths for LL-37, KR-12, and RI-10-treated Δ*mgrB* cells were higher than the corresponding
257 values obtained for the wild type by 2.5-, 2.3-, and 1.9-fold, respectively; however, there is no
258 difference in cell length in the KE-10-treated cells (Figures 4D-E), indicating a central role of the
259 RI-10 containing LL-37 segments in activation in the absence of *mgrB*.
260 It is known that high stimulation of PhoQ from exposure to LL-37 results in differential regulation
261 of specific PhoP-regulated promoters, including that of *mgrB* (29). Also, upon activation by LL-
262 37, a mutated *mgrB-t7a* promoter (with a T7A substitution in the PhoP-binding site) shows a
263 higher fold change in transcriptional activity relative to the wild-type *mgrB* promoter. To
264 substantiate whether there may be an increased transcriptional response to peptide treatment
265 via this promoter, we analyzed wild-type and Δ*mgrB* strains carrying the *mgrB-t7a* promoter. We
266 observed a significant increase in cell size heterogeneity in wild-type cells treated with LL-37
267 and KR-12, and Δ*mgrB* cells treated with LL-37, KR-12, and RI-10 (Figure S2). The cells did not

268 display an increase in cell length when treated with control peptide KE-10 or in the absence of a
269 peptide. If the exacerbated cell elongation observed in peptide-treated Δ*mgrB* cells is indeed
270 due to a PhoQP-dependent mechanism that is mediated by QueE, we should see this
271 phenotype suppressed upon deletion of *queE*. Consistent with our hypothesis, Δ*mgrB* Δ*queE*
272 cells treated with LL-37, KR-12, and RI-10 did not show an increase in PhoQ-dependent
273 transcriptional reporter activity and displayed a loss of filamentation and a decrease in cell size
274 heterogeneity (Figure S3). Together, these data suggest that LL-37 and its derivatives bind and
275 actively stimulate PhoQ. In the absence of MgrB, these peptides further enhance PhoQ
276 activation. Importantly, cell elongation serves as a sensitive phenotype for peptide-mediated
277 PhoQ stimulation in *E. coli*. Wild-type cells exposed to sub-MIC peptide concentrations exhibit
278 moderate elongation, reflecting intermediate PhoQ activity, while *ΔmgrB* cells display
279 significantly increased cell lengths, indicating robust PhoQ activation (Figure 4E).
280

281 ## Discussion

282 Despite extensive investigation, fundamental questions remain about the molecular
283 mechanisms of peptide-mediated signal transduction by the PhoQ-PhoP system. Moreover, the
284 effects of PhoPQ activation by cationic AMPs in cells and the physiological importance of these
285 interactions have not been elucidated. We address two critical questions in this work: (i) Can
286 peptides lacking potent antimicrobial activity still interact with PhoQ and act as a signal for this
287 pathway? Using LL-37 and derivatives with variable MICs and antibacterial activities against *E.*
288 *coli* cells, we show that the signaling function of peptides through the PhoQ-PhoP system is
289 separable from their antimicrobial activity (Figure 5A), suggesting that bacteria may use this
290 pathway primarily as a detection mechanism for host environments rather than simply as a
291 response to membrane damage. (ii) Do the peptides actively stimulate PhoQ, or do they exert
292 their effect on PhoQ passively by displacing the inhibitor protein, MgrB? Many studies on

293 peptide-induced signaling of PhoQ measure the activity of peptides using PhoP-dependent
294 transcriptional reporters as a proxy. In agreement with the previous studies, upon exposure to
295 peptides, we do not observe a significant increase in PhoQP-driven transcriptional reporter
296 activity in *ΔmgrB* cells relative to the wild type. It is possible that the derepression of PhoP-
297 regulated gene expression in the absence of MgrB could lead to lower sensitivity of the reporter
298 signal, masking small increments in the amplitude. While such reporters are incredibly useful in
299 determining the activation status of this pathway and measuring the transcription levels, we
300 have a second, sensitive readout – a cell elongation or filamentation phenotype in response to
301 peptide stress in *E. coli*. Based on our microscopy and cell length measurements, we find that
302 cells elongate significantly upon exposure to sublethal concentrations of peptides, LL-37 and
303 KR-12, even though the promoter reporters do not show a significant change in their activities.
304 The extent of cell elongation may differ in response to specific peptides, as we note that
305 filamentation induced by an AMP, C18G, in wild-type *E. coli* cells is quite robust, with an
306 average cell length of > 20 μm (2). Upon deletion of MgrB, the average cell lengths increased
307 further, and even RI-10-treated cells displayed cell elongation; this observation suggests that
308 AMPs may activate PhoQ directly in addition to causing MgrB dissociation as proposed
309 previously (23). Our findings elucidate PhoQ-dependent effects of these peptides and support a
310 model where peptides play an active and direct role in PhoQ activation (Figure 5B).
311
312 Our understanding of what characteristics of AMPs are required to activate the PhoP-PhoQ
313 system is still evolving. A previous report found a correlation between the extent of positive
314 charge, hydrophobicity, and amphipathicity of an AMP and its ability to activate PhoQ-PhoP (8).
315 Intriguingly, the authors discovered that even a peptide with minimal positive charge (+1) but
316 containing histidines was highly potent at activating the system, suggesting the existence of an
317 activation mechanism more complex than thought. A later study with 117 AMPs from the
318 Antimicrobial Peptide Database (30) showed that PhoQ is activated by a diverse set of AMPs,

319 including the human cathelicin LL-37 and non-cathelicidin peptides that carry either an α-helical
320 or a combination of α-helical/β-sheet structural regions (31). In our work, we see that LL-37
321 derivatives induce PhoQ-dependent morphological changes, and KR-12, the smallest
322 antibacterial peptide, is also the smallest peptide sequence for the PhoPQ induction. Further,
323 RI-10, but not KE-10, became responsive upon the deletion of *mgrB*. Interestingly, LL-25, the N-
324 terminal segment of LL-37 which does not kill bacteria under normal conditions (31), does not
325 activate PhoPQ based on the recent human AMPs screen study although it contains partial
326 sequence of KR-12 (30). LL-25 can be obtained by extending the sequence of KE-10 from both
327 ends (Tables S2, S3). Together, the data from the current study suggest that part of the LL-37
328 amino acid sequence that overlaps with both KR-12 and RI-10 is likely mediating the interaction
329 with PhoQ. More broadly, our findings imply that the bacterial molecular detection machinery is
330 elegantly tuned to specifically target the core antimicrobial region of human antimicrobial
331 peptide LL-37 but not fragments outside this region. When broadly viewed from the host-
332 pathogen interaction at the molecular level, bacterial detection of the core antimicrobial region of
333 human cathelicidin LL-37 (24) is remarkably efficient since this region is commonly shared by all
334 the active fragments of LL-37 naturally produced in human skin (Table S3), including KS-27,
335 KR-20, KS-30, RK-31, and LL-29 (32). Indeed, all these human cathelicidin fragments
336 responded to the PhoPQ system based on a recent screening of human AMPs registered in the
337 APD (30). Collectively, these findings underscore that the bacterial PhoQ-PhoP system likely
338 senses host defense peptides based on evolutionarily conserved structural and chemical
339 properties independent of their antimicrobial activity, allowing bacteria to mount preemptive
340 responses rather than simply react to membrane damage.
341
342 Finally, the dramatic rise of antimicrobial resistance is a major public health concern. AMPs and
343 other peptide derivatives are relatively small, typically comprised of around 10 to 50 amino acids
344 (30), and constitute a key component of host innate immunity for defense against microbial

345 pathogens (32, 33). These cationic peptides are relatively cheap to produce, have good thermal
346 stability and water solubility, and exhibit a broad spectrum of activity against bacteria and fungi,
347 making them promising candidates for drug development (34–38). Studying the bacterial
348 responses to antimicrobial peptides in general provides us with a fundamental understanding of
349 how pathogens can sense, adapt, and develop tolerance to these host defense molecules and
350 guide the strategic design of novel therapeutics with enhanced efficacy to overcome the growing
351 antibiotic resistance problem.
352

353 Materials and Methods

354 Strains

355 Details of the strains used in this study are provided in Table S4. AML20, JNC21, NRS5, NRS6,
356 SAM31, TIM92, TIM100, and TIM166 are *E. coli* K-12 MG1655 derivatives. Additionally, clinical
357 strains of *E. coli*, E423-17, E416-17, and ATCC strain 25922 were used for specific assays as
358 indicated. NRS6 was made by transducing the KEIO strain JW1815 into the TIM148 and
359 TIM166 strains, respectively, using $P1_{vir}$.
360

361 Media, reagents, and growth conditions

362 Routine bacterial growth on solid agar was performed using LB Miller medium (IBI Scientific)
363 containing 1.5% bacteriological grade agar (VWR Lifesciences) at 37°C. Liquid cultures were
364 grown at 37°C with aeration in either LB miller medium or minimal A medium (MinA) (39)
365 (K_2HPO_4 (10.5 g l^{-1}), KH_2PO_4 (4.5 g l^{-1}), $(NH_4)_2SO_4$ (1.0 g l^{-1}), Na_3 citrate.$2H_2O$ (0.5 g l^{-1}),
366 supplemented with 0.1% casamino acids, 0.2% glucose and 1 mM $MgSO_4$ unless otherwise
367 indicated. Throughout this study, supplemented MinA, as indicated above, will be referred to as
368 a minimal medium. In addition, Mueller-Hinton broth (MHB, catalog info) and tryptic soy broth

369 (TSB, catalog info) were used for minimum inhibitory/bactericidal concentration (MIC/MBC)
370 assays. Peptides and/or AMPs used in the study are indicated in Table S2.
371
372 For the measurement of cell length and transcriptional reporter activity, overnight cultures of
373 SAM31, TIM92, TIM100, AML20, SAA58, and JNC21 were grown in supplemented MinA
374 containing 1 mM $MgSO_4$. Saturated cultures were back diluted 1:500 into 5 ml supplemented
375 MinA with 0.1 mM Mg^{2+} and grown for 2 hours in a shaker at 300 rpm. Each culture was split
376 into two tubes, with one tube designated as a no-peptide control and the second tube where a
377 test peptide was added. LL-37, KR-12, RI-10, and KE-10 were added to a final concentration of
378 1.25 μM, 5 μM, 5 μM, and 5 μM, respectively. These cultures were further grown for 4 hours at
379 37°C in a roller drum at 60 rpm.
380
381 **Microscopy and image analysis**
382 Cell morphology was observed and single-cell fluorescence to measure transcriptional reporter
383 activity was performed using phase contrast and fluorescence microscopy as previously
384 described (2). 3 μl of the cells were immobilized on a 1% agarose pad and observed using a
385 Nikon TiE fluorescent microscope with a TI2-S-HU attachable mechanical stage and a perfect
386 focus system (PFS). The images were captured using a Teledyne Photometrics Prime 95B
387 sCMOS camera with 1x1 binning. YFP and CFP fluorescence was imaged using a 100 ms
388 exposure time at 20% intensity. Image acquisition was done using Metamorph software version
389 7.10.3.279 (Molecular Devices, Sunnyvale, CA). The background fluorescence was determined
390 using MG1655 cells grown under the same conditions. The average cell fluorescence was
391 quantified using ImageJ (40) and the MicrobeJ plugin (41). Data from independent replicates
392 were plotted using R.
393
394

395 **Minimum inhibitory/bactericidal concentration (MIC/MBC) testing**

396 The antibacterial activity of the peptides against *E. coli* MG1655, E423-17, E416-17, and 25922
397 strains was evaluated using a previously established protocol (42). Briefly, a peptide
398 concentration gradient with twofold dilution was prepared in the 96-well polystyrene microplate
399 at 10 µl per well. Bacteria were grown to the exponential phase in MHB, TSB, or supplemented
400 MinA. It was then diluted to ~10^5 CFU/ml in MHB, TSB, or supplemented MinA with 0.1 mM
401 $MgSO_4$, and partitioned into the 96-well microplate at 90 µl per well. After overnight incubation at
402 37°C, readings were taken at 600 nm using a ChroMate 4300 Microplate Reader at (GMI,
403 Ramsey, MN). The minimum inhibitory concentration (MIC), represented as ranges, was
404 determined for wells without bacterial growth. For minimum bactericidal concentration (MBC)
405 determination, aliquots of 30 µl from growth-absent wells were plated on MH agar plates, and
406 the lowest peptide concentration with no isolated colony was considered the MBC. Results were
407 expressed in µM.

408

409 **Membrane permeabilization**

410 The peptide ladder was prepared as described for the antibacterial assay in a black COSTAR
411 96-well plate. Propidium iodide (PI) (MP Biomedicals, Solon, OH) was prepared in the dark and
412 dissolved in DMSO (Thermo Fisher Scientific, NY) to 20 mM. This PI stock solution was further
413 diluted to 1 mM with water and 2 µl of 1 mM PI was added to each well. An overnight culture of
414 *E. coli* K12 MG1655 was inoculated into 1xMinA supplemented with 0.2% glucose, 0.1%
415 casamino acids, 0.1mM $MgSO_4$, and grown to exponential phase. It was then diluted to OD_{600}
416 0.11 in the same media, and 88 µl was added to each well. The plate was incubated at 37℃ with
417 continuous shaking in a FLUOstar Omega (BMG LABTECH, NC) microplate reader. The sample
418 was read every 5 minutes for 24 cycles with excitation and emission wavelengths of 584 nm and
419 620 nm, respectively.

420

421 **Killing kinetics**

422 *E. coli* K12 MG1655 was grown to the exponential phase (OD_{600} ~ 0.3) in 1xMinA supplemented
423 with 0.2% glucose, 0.1% casamino acids, 1 mM $MgSO_4$. The culture was diluted to OD_{600} 0.001
424 (~10^5 CFU/ml) in 1xMinA supplemented with 0.2% glucose, 0.1% casamino acids, 0.1mM
425 $MgSO_4$. One milliliter of bacterial suspension was then mixed with LL-37 (4 μM, 2× MIC), KR-12
426 (8 μM, 2× MIC) or RI-10 (32 μM) and incubated at 37°C. After 15, 30, 60, 90, and 120 minutes
427 of incubation, 50 μl was taken and serially diluted with 1×PBS. Then, 50 μl of the diluted
428 suspension was plated on MH agar Agar plates. The plates were incubated overnight at 37°C
429 for bacterial CFU determination.

430

431 **Membrane depolarization**

432 An overnight culture of *E. coli* K12 MG1655 was inoculated into 1xMinA supplemented with
433 0.2% glucose, 0.1% casamino acids, 1 mM $MgSO_4$, and grown to exponential phase. Bacteria
434 were washed with 1×PBS, re-suspended in twice the volume of 1×PBS containing 25 mM
435 glucose, and incubated at 37°C for 15 minutes. Then, 500 nM (final concentration) of the
436 DiBAC4 (3) bis-(1,3-dibutylbarbituric acid) trimethine oxonol (ANASPEC, CA) was added and
437 vortexed gently. Aliquots of 90 μl of the energized bacteria solution were loaded to the 96 well
438 plates (Corning COSTAR, AZ) and placed in a FLUOstar Omega microplate reader (BMG
439 LABTECH, NC). Fluorescence was read for 15 min at excitation and emission wavelengths of
440 485 nm and 520 nm, respectively. Then, 10 μl of peptide solutions were added and fluorescence
441 readings were recorded for 45 min. Triton X-100 (0.1%) was used as a positive control.

442

443 **Acknowledgments**

444 The authors thank Dr. Mark Goulian for sharing transcriptional reporter strains for *mgrB*, Dr.
445 Nitish Sharma for preparing *ΔmgrB* strains carrying the reporters, Dr. Premal Shah for critical
446 feedback and assistance with data visualization and figure creation, Dr. Manuela Roggiani for

critical feedback on the manuscript, and members of the Yadavalli and Wang labs for helpful discussions.

Funding

S.S.Y. is supported by the National Institutes of Health - National Institute of General Medical Sciences (NIH-NIGMS) ESI-MIRA R35 GM147566 and institutional start-up funds from Rutgers. A.M. is supported by the Waksman Institute Busch Predoctoral fellowship (2024-25) at Rutgers. G.W. is supported by the NIH/NIAID R56 AI175209. The funders did not play any role in the study design, data collection and analysis, decision to publish, or preparation of the manuscript.

Author contributions

S.S.Y. and G.W. conceived the experiments. All authors planned the experiments, designed the methodology, and performed data analysis. S.A.A., A.F.M., and A.M. performed the experiments. All authors contributed to the writing and editing of the manuscript.

Competing interests

The authors declare no competing financial interests.

Materials and resource availability

Requests for strains and plasmids generated in this study should be directed to and will be fulfilled by the lead contact, Srujana S. Yadavalli (sam.yadavalli@rutgers.edu). Further information and requests for resources and reagents should be directed to and will be fulfilled by Srujana S. Yadavalli (sam.yadavalli@rutgers.edu) and Guangshun Wang (gwang@unmc.edu).

473 **Data availability**

474 The main manuscript and its supporting files include all data generated or analyzed during this

475 study.

476

477 ## References

478 1. M. W. Bader, *et al.*, Recognition of antimicrobial peptides by a bacterial sensor kinase. *Cell* **122**, 461–
479 472 (2005).

480 2. S. S. Yadavalli, *et al.*, Antimicrobial peptides trigger a division block in Escherichia coli through
481 stimulation of a signalling system. *Nat. Commun.* **7**, 12340 (2016).

482 3. E. A. Groisman, The pleiotropic two-component regulatory system PhoP-PhoQ. *J. Bacteriol.* **183**,
483 1835–1842 (2001).

484 4. J. Yuan, F. Jin, T. Glatter, V. Sourjik, Osmosensing by the bacterial PhoQ/PhoP two-component
485 system. *Proc. Natl. Acad. Sci. U. S. A.* **114**, E10792–E10798 (2017).

486 5. S. Matamouros, S. I. Miller, S. Typhimurium strategies to resist killing by cationic antimicrobial
487 peptides. *Biochim. Biophys. Acta* **1848**, 3021–3025 (2015).

488 6. Z. D. Dalebroux, S. I. Miller, Salmonellae PhoPQ regulation of the outer membrane to resist innate
489 immunity. *Curr. Opin. Microbiol.* **17**, 106–113 (2014).

490 7. R. K. Ernst, T. Guina, S. I. Miller, Salmonella typhimurium outer membrane remodeling: role in
491 resistance to host innate immunity. *Microbes Infect.* **3**, 1327–1334 (2001).

492 8. T. Shprung, A. Peleg, Y. Rosenfeld, P. Trieu-Cuot, Y. Shai, Effect of PhoP-PhoQ activation by broad
493 repertoire of antimicrobial peptides on bacterial resistance. *J. Biol. Chem.* **287**, 4544–4551 (2012).

494 9. M. F. Burton, P. G. Steel, The chemistry and biology of LL-37. *Nat. Prod. Rep.* **26**, 1572–1584 (2009).

495 10. D. Vandamme, B. Landuyt, W. Luyten, L. Schoofs, A comprehensive summary of LL-37, the factotum
496 human cathelicidin peptide. *Cell. Immunol.* **280**, 22–35 (2012).

497 11. G. Wang, *et al.*, Design of antimicrobial peptides: Progress made with human cathelicidin LL-37. *Adv.*
498 *Exp. Med. Biol.* **1117**, 215–240 (2019).

499 12. F. Lu, Y. Zhu, G. Zhang, Z. Liu, Renovation as innovation: Repurposing human antibacterial peptide
500 LL-37 for cancer therapy. *Front. Pharmacol.* **13**, 944147 (2022).

501 13. K. Niemirowicz, *et al.*, Magnetic nanoparticles enhance the anticancer activity of cathelicidin LL-37
502 peptide against colon cancer cells. *Int. J. Nanomedicine* **10**, 3843–3853 (2015).

503 14. K. Kuroda, K. Okumura, H. Isogai, E. Isogai, The human cathelicidin antimicrobial peptide LL-37 and
504 mimics are potential anticancer drugs. *Front. Oncol.* **5**, 144 (2015).

505 15. S. Tripathi, *et al.*, Antiviral activity of the human cathelicidin, LL-37, and derived peptides on seasonal
506 and pandemic influenza A viruses. *PLoS One* **10**, e0124706 (2015).

507 16. I. Ginsburg, Bactericidal cationic peptides can also function as bacteriolysis-inducing agents
508 mimicking beta-lactam antibiotics?; it is enigmatic why this concept is consistently disregarded. *Med.*
509 *Hypotheses* **62**, 367–374 (2004).

17. Y. Zhang, J. Lakshmaiah Narayana, Q. Wu, X. Dang, G. Wang, Structure and activity of a selective antibiofilm peptide SK-24 derived from the NMR structure of human cathelicidin LL-37. *Pharmaceuticals (Basel)* **14**, 1245 (2021).

18. K. A. Henzler Wildman, D.-K. Lee, A. Ramamoorthy, Mechanism of lipid bilayer disruption by the human antimicrobial peptide, LL-37. *Biochemistry* **42**, 6545–6558 (2003).

19. J. Turner, Y. Cho, N. N. Dinh, A. J. Waring, R. I. Lehrer, Activities of LL-37, a cathelin-associated antimicrobial peptide of human neutrophils. *Antimicrob. Agents Chemother.* **42**, 2206–2214 (1998).

20. A. M. Lippa, M. Goulian, Feedback inhibition in the PhoQ/PhoP signaling system by a membrane peptide. *PLoS Genet.* **5**, e1000788 (2009).

21. M. E. Salazar, A. I. Podgornaia, M. T. Laub, The small membrane protein MgrB regulates PhoQ bifunctionality to control PhoP target gene expression dynamics. *Mol. Microbiol.* **102**, 430–445 (2016).

22. S. S. Yadavalli, *et al.*, Functional determinants of a small protein controlling a broadly conserved bacterial sensor kinase. *J. Bacteriol.* **202** (2020).

23. S. Jiang, *et al.*, The inhibitory mechanism of a small protein reveals its role in antimicrobial peptide sensing. *Proc. Natl. Acad. Sci. U. S. A.* **120**, e2309607120 (2023).

24. G. Wang, Structures of human host defense cathelicidin LL-37 and its smallest antimicrobial peptide KR-12 in lipid micelles. *J. Biol. Chem.* **283**, 32637–32643 (2008).

25. K. Chen, W. Gong, J. Huang, T. Yoshimura, J. M. Wang, The potentials of short fragments of human anti-microbial peptide LL-37 as a novel therapeutic modality for diseases. *Front. Biosci. (Landmark Ed.)* **26**, 1362–1372 (2021).

26. J. Lakshmaiah Narayana, *et al.*, Origami of KR-12 designed antimicrobial peptides and their potential applications. *Antibiotics (Basel)* **13**, 816 (2024).

27. N. Mookherjee, M. A. Anderson, H. P. Haagsman, D. J. Davidson, Antimicrobial host defence peptides: functions and clinical potential. *Nat. Rev. Drug Discov.* **19**, 311–332 (2020).

28. S. A. Adeleye, S. S. Yadavalli, Queuosine biosynthetic enzyme, QueE moonlights as a cell division regulator. *PLoS Genet.* **20**, e1011287 (2024).

29. T. Miyashiro, M. Goulian, Stimulus-dependent differential regulation in the Escherichia coli PhoQ PhoP system. *Proc. Natl. Acad. Sci. U. S. A.* **104**, 16305–16310 (2007).

30. G. Wang, X. Li, Z. Wang, APD6: the antimicrobial peptide database is expanded to promote research and development by deploying an unprecedented information pipeline. *Nucleic Acids Res.* **in Press** (2025).

31. K. R. Brink, *et al.*, An E. coli display method for characterization of peptide-sensor kinase interactions. *Nat. Chem. Biol.* **19**, 451–459 (2023).

32. G. Wang, *et al.*, Structure, dynamics, and antimicrobial and immune modulatory activities of human LL-23 and its single-residue variants mutated on the basis of homologous primate cathelicidins. *Biochemistry* **51**, 653–664 (2012).

33. M. Murakami, B. Lopez-Garcia, M. Braff, R. A. Dorschner, R. L. Gallo, Postsecretory processing generates multiple cathelicidins for enhanced topical antimicrobial defense. *J. Immunol.* **172**, 3070–3077 (2004).

34. G. Laverty, S. P. Gorman, B. F. Gilmore, The potential of antimicrobial peptides as biocides. *Int. J. Mol. Sci.* **12**, 6566–6596 (2011).

35. L. Segev-Zarko, M. L. Mangoni, Y. Shai, "Antimicrobial peptides: multiple mechanisms against a variety of targets" in *Antimicrobial Peptides: Discovery, Design and Novel Therapeutic Strategies*, (CABI, 2017), pp. 119–134.

36. R. E. W. Hancock, K. L. Brown, N. Mookherjee, Host defence peptides from invertebrates--emerging antimicrobial strategies. *Immunobiology* **211**, 315–322 (2006).

37. T. L. Raguse, E. A. Porter, B. Weisblum, S. H. Gellman, Structure-activity studies of 14-helical antimicrobial beta-peptides: probing the relationship between conformational stability and antimicrobial potency. *J. Am. Chem. Soc.* **124**, 12774–12785 (2002).

38. D. L. Lee, R. S. Hodges, Structure-activity relationships of de novo designed cyclic antimicrobial peptides based on gramicidin S. *Biopolymers* **71**, 28–48 (2003).

39. J. H. Miller, *A Short Course in Bacterial Genetics*, 1987th Ed. (Cold Spring Harbor Laboratory Press, 1992).

40. C. A. Schneider, W. S. Rasband, K. W. Eliceiri, NIH Image to ImageJ: 25 years of image analysis. *Nat. Methods* **9**, 671–675 (2012).

41. A. Ducret, E. M. Quardokus, Y. V. Brun, MicrobeJ, a tool for high throughput bacterial cell detection and quantitative analysis. *Nat. Microbiol.* **1**, 16077 (2016).

42. B. Mishra, T. Lushnikova, R. M. Golla, X. Wang, G. Wang, Design and surface immobilization of short anti-biofilm peptides. *Acta Biomater.* **49**, 316–328 (2017).

Figure legends

Figure 1. Membrane permeabilization (A-C) and depolarization (D-F) activity of a series of LL-37, KR-12, and RI-10 in *E. coli* K-12 MG1655. The assay was performed in supplemented MinA with 0.1 mM $MgSO_4$. RFU: Relative fluorescence intensity. Data are represented as mean ± range for two independent replicates.

Figure 2. PhoQP-regulated transcription and cell morphology of *E. coli* cells treated with sub-MIC levels of antimicrobial peptides. (A) PhoQP-dependent promoter P_{mgrB}-*yfp* reporter activity, **(B)** phase contrast micrographs, and **(C)** quantification of cell lengths of *E. coli* MG1655 (TIM92) cells grown in the presence of sub-MIC levels of antimicrobial peptides LL-37 (1.25 μM), KR-12 (5 μM), RI-10 (5 μM), and KE-10 (5 μM) in supplemented MinA with 0.1 mM $MgSO_4$. Data are obtained from at least three biological replicates; mean and median values are shown in red text and black bars, respectively. The number of cells analyzed is indicated for each

583 sample. P-values indicate the results of a Student's t-test: ****P ≤ 0.0001, *P ≤ 0.05, and "ns" =
584 P > 0.05. Scale bar = 5 μm.

585 **Figure 3. PhoQP-regulated transcription and cell morphology of Δ*queE* and Δ*phoQ* cells**
586 **treated with sub-MIC levels of antimicrobial peptides. (A)** Phase contrast micrographs, **(B,**
587 **D)** PhoQP-dependent promoter P_{mgrB}-*yfp* reporter activity, and **(C, E)** quantification of cell
588 lengths of Δ*phoQ* (TIM100) cells and Δ*queE* (SAM31) cells grown in the presence of sub-MIC
589 levels of the antimicrobial peptides LL-37 (1.25 μM), KR-12 (5 μM), RI-10 (5 μM), and KE-10 (5
590 μM) in supplemented MinA with 0.1 mM $MgSO_4$. Data are obtained from at least three biological
591 replicates; mean and median values are shown in red text and black bars, respectively. The
592 number of cells analyzed is indicated for each sample. P-values indicate the results of a
593 Student's t-test: ****P ≤ 0.0001, ***P ≤ 0.001, *P ≤ 0.05, and "ns" = P > 0.05. Scale bar = 5 μm.

594 **Figure 4. PhoQP-regulated transcription and cell morphology of Δ*mgrB* cells treated with**
595 **sub-MIC levels of antimicrobial peptides. (A)** PhoQP-dependent promoter P_{mgrB}-*yfp* reporter
596 activity in Δ*mgrB* (AML20) cells, **(B)** comparison of PhoQP-dependent promoter P_{mgrB}-*yfp*
597 reporter activity in Δ*mgrB* (AML20) cells with that of WT *E. coli* (TIM92) from Fig. 2A, and **(C)**
598 phase contrast micrographs of WT *E. coli* (TIM92) and Δ*mgrB* (AML20) cells, **(D)** quantification
599 of cell lengths of Δ*mgrB* (AML20) cells, and **(E)** comparison of cell lengths in Δ*mgrB* (AML20)
600 cells with that of WT *E. coli* (TIM92) from Fig. 2C. Cells were grown in the presence of sub-MIC
601 levels of the antimicrobial peptides LL-37 (1.25 μM), KR-12 (5 μM), RI-10 (5 μM), and KE-10 (5
602 μM) in supplemented MinA with 0.1 mM $MgSO_4$. Arrows in panel (E) indicate the PhoQ
603 activation status. Data are obtained from at least three biological replicates; mean and median
604 values are shown in red text and black bars, respectively. The number of cells analyzed is
605 indicated for each sample. P-values indicate the results of a Student's t-test: ****P ≤ 0.0001, **P
606 ≤ 0.01, *P ≤ 0.05, and "ns" = P > 0.05. Scale bar = 5 μm.

607 **Figure 5. Schematic overview of peptide stress response through the *E. coli* PhoQ-PhoP**
608 **signaling system. (A)** At high concentrations, antimicrobial peptides affect membrane integrity

609 and cause damage, leading to cell death. At sub-MIC levels, peptides are sensed by the
610 signaling systems, such as PhoQ/PhoP, which control the gene expression under peptide
611 stress, leading to physiological changes, including cell elongation and modification of the outer
612 cell membrane. **(B)** At physiological magnesium concentration, PhoQ is strongly stimulated by
613 specific cationic peptides, and some PhoQ molecules are inhibited by the small protein
614 regulator, MgrB, leading to an intermediate level of PhoQ activation. In the absence of MgrB,
615 PhoQ is not inhibited, and when cells are exposed to peptides, PhoQ is strongly activated,
616 resulting in maximal activation of this signaling system.
617
618
619
620
621
622
623
624
625
626
627
628
629
630
631
632
633

634 ## Tables and Figures

635

636 **Table 1. Minimum inhibitory concentration (MIC) and minimum bactericidal concentration**
637 **(MBC) values for LL-37 and its derivatives against *E. coli* K-12 MG1655**. MIC values (μM) of
638 antimicrobial peptide LL-37 and its derivatives KR-12, RI-10, and KE-10 against *E. coli* K-12
639 MG1655 in supplemented minimal medium (Min A), Mueller Hinton broth (MHB), and tryptic soy
640 broth (TSB). The corresponding MBC values (μM) are shown within parentheses. Gentamicin is
641 included as a bactericidal antibiotic control. Data represent values obtained from three
642 independent biological replicates.

Strain	Media	LL-37	KR-12	RI-10	KE-10	Gentamicin
E. coli K-12 MG1655	Min A	2 (2)	8-16 (16)	>64 (>64)	>64 (>64)	0.5-1 (1)
	MHB	8 (8)	16-32 (32)	>64 (>64)	>64 (>64)	0.5-1 (1)
	10% MHB	2 (4)	2 (2)	>64 (>64)	>64 (>64)	ND
	TSB	8 (16)	16 (32)	>64 (>64)	>64 (>64)	1-2 (2)
E. coli K-12 MG1655 Δ*mgrB*	Min A	2 (2)	8 (16)	>64 (>64)	>64 (>64)	-
	MHB	8 (8)	8-16 (16)	>64 (>64)	>64 (>64)	-
	10% MHB	2 (2)	2 (2)	>64 (>64)	>64 (>64)	-
	TSB	8-16 (32)	16 (32)	>64 (>64)	>64 (>64)	-

Figure 1

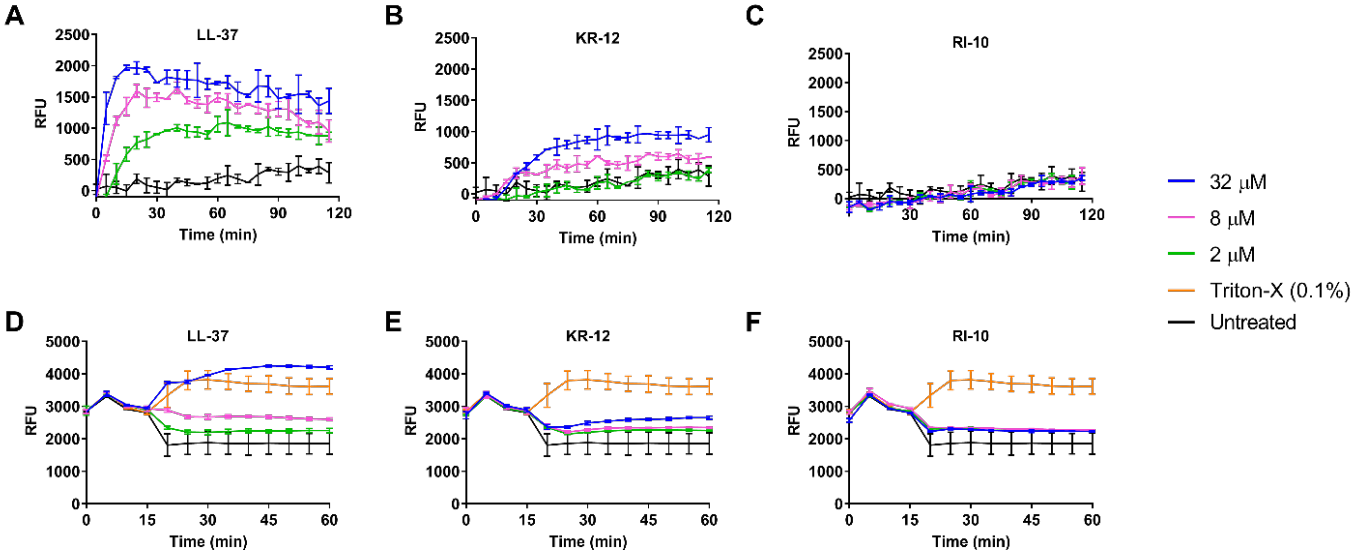
A
LL-37
RFU
Time (min)
B
KR-12
RFU
Time (min)
C
RI-10
RFU
Time (min)
D
LL-37
RFU
Time (min)
E
KR-12
RFU
Time (min)
F
RI-10
RFU
Time (min)
32 μM
8 μM
2 μM
Triton-X (0.1%)
Untreated

Figure 2

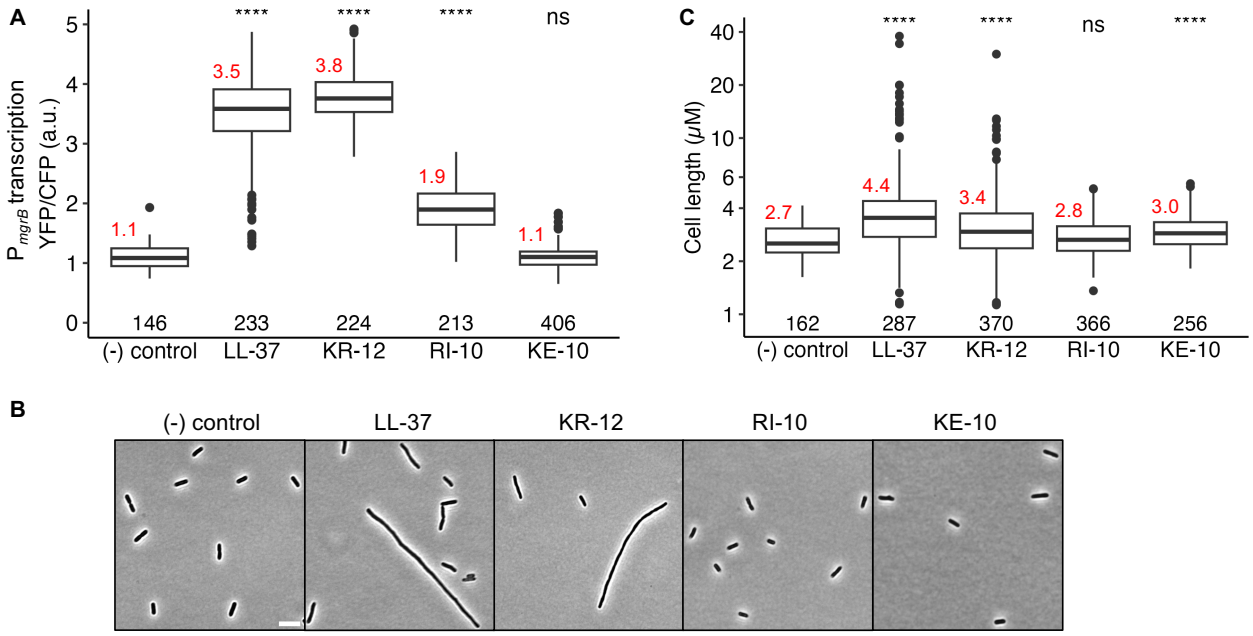
A
P_{mgrB} transcription YFP/CFP (a.u.)
5
4
3
2
1
0
1.1
3.5
3.8
1.9
1.1
****
****
****
ns
146
233
224
213
406
(-) control
LL-37
KR-12
RI-10
KE-10
C
Cell length (μM)
40
20
10
6
4
2
1
2.7
4.4
3.4
2.8
3.0
****
****
ns
****
162
287
370
366
256
(-) control
LL-37
KR-12
RI-10
KE-10
B
(-) control
LL-37
KR-12
RI-10
KE-10

Figure 3

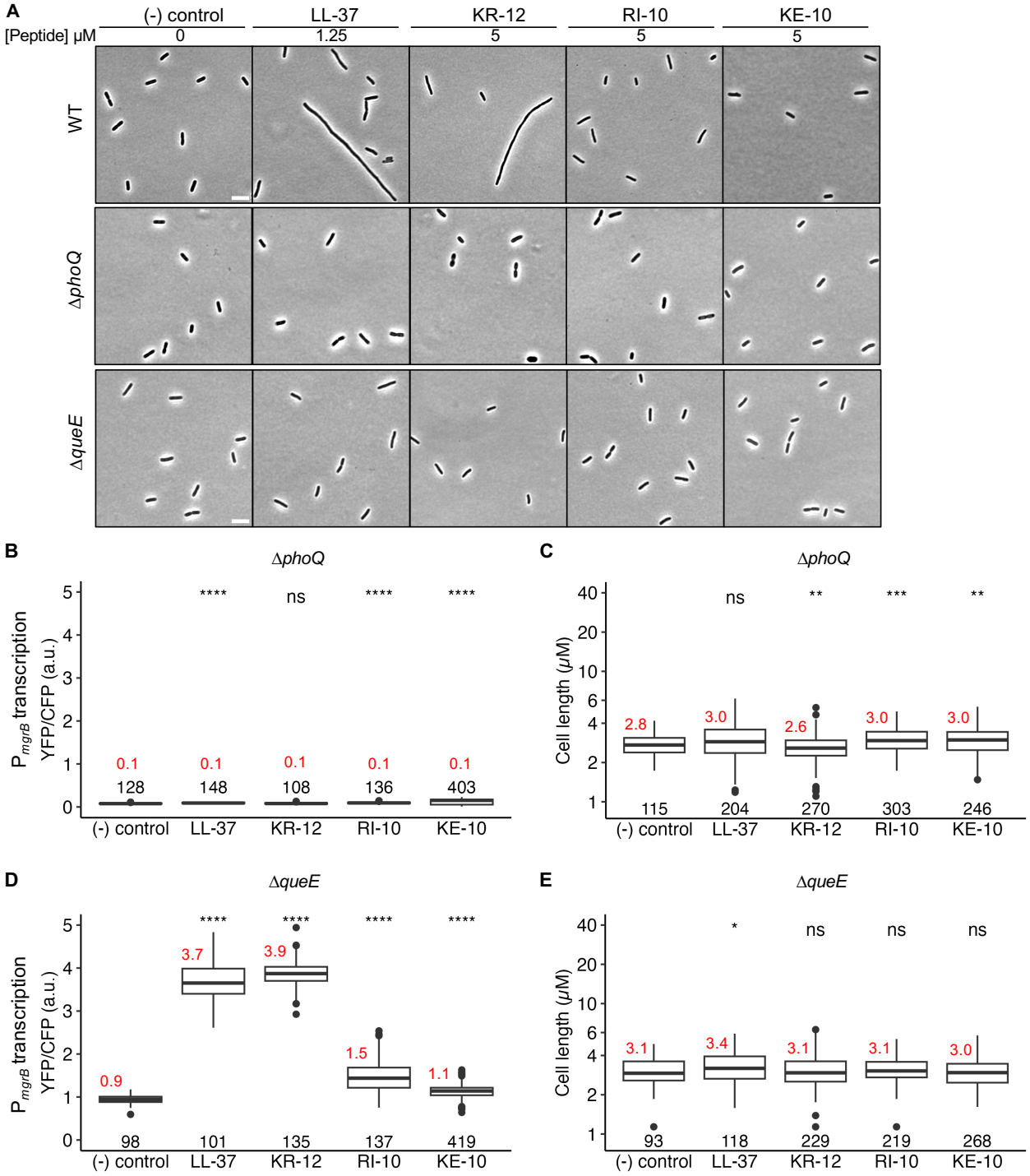
A
(-) control
LL-37
KR-12
RI-10
KE-10
[Peptide] μM
0
1.25
5
5
5
WT
ΔphoQ
ΔqueE
B
ΔphoQ
P_mgrB transcription
YFP/CFP (a.u.)
****
ns
****
****
0.1
0.1
0.1
0.1
0.1
128
148
108
136
403
(-) control
LL-37
KR-12
RI-10
KE-10
C
ΔphoQ
Cell length (μM)
ns
**
***
**
2.8
3.0
2.6
3.0
3.0
115
204
270
303
246
(-) control
LL-37
KR-12
RI-10
KE-10
D
ΔqueE
P_mgrB transcription
YFP/CFP (a.u.)
****
****
****
****
0.9
3.7
3.9
1.5
1.1
98
101
135
137
419
(-) control
LL-37
KR-12
RI-10
KE-10
E
ΔqueE
Cell length (μM)
*
ns
ns
ns
3.1
3.4
3.1
3.1
3.0
93
118
229
219
268
(-) control
LL-37
KR-12
RI-10
KE-10

Figure 4

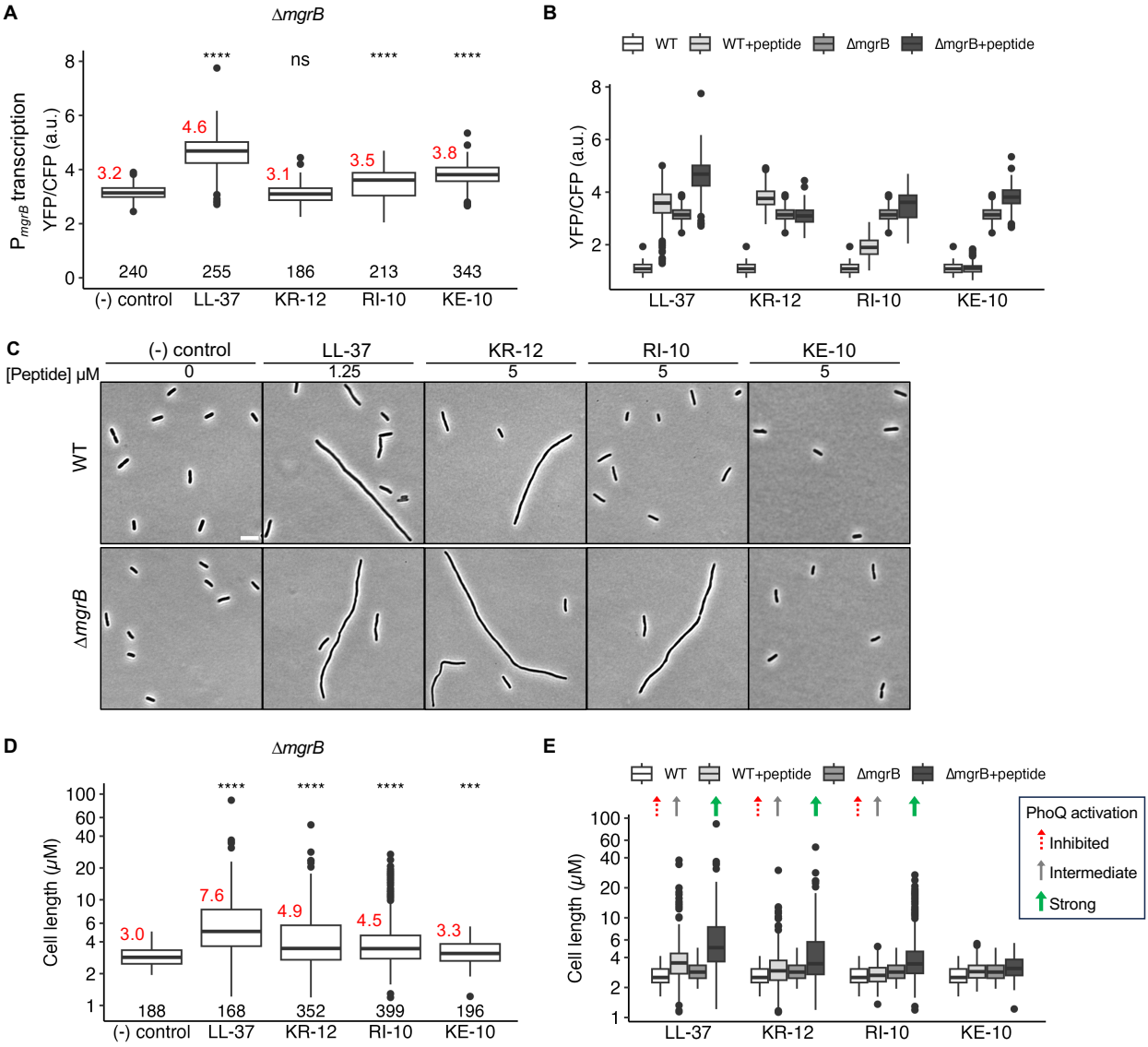
A
ΔmgrB
P_{mgrB} transcription
YFP/CFP (a.u.)
****
ns
****
****
3.2
4.6
3.1
3.5
3.8
240
255
186
213
343
(-) control
LL-37
KR-12
RI-10
KE-10
B
WT
WT+peptide
ΔmgrB
ΔmgrB+peptide
YFP/CFP (a.u.)
LL-37
KR-12
RI-10
KE-10
C
(-) control
LL-37
KR-12
RI-10
KE-10
[Peptide] μM
0
1.25
5
5
5
WT
ΔmgrB
D
ΔmgrB
Cell length (μM)
****
****
****
***
3.0
7.6
4.9
4.5
3.3
188
168
352
399
196
(-) control
LL-37
KR-12
RI-10
KE-10
E
WT
WT+peptide
ΔmgrB
ΔmgrB+peptide
Cell length (μM)
PhoQ activation
Inhibited
Intermediate
Strong
LL-37
KR-12
RI-10
KE-10

Figure 5

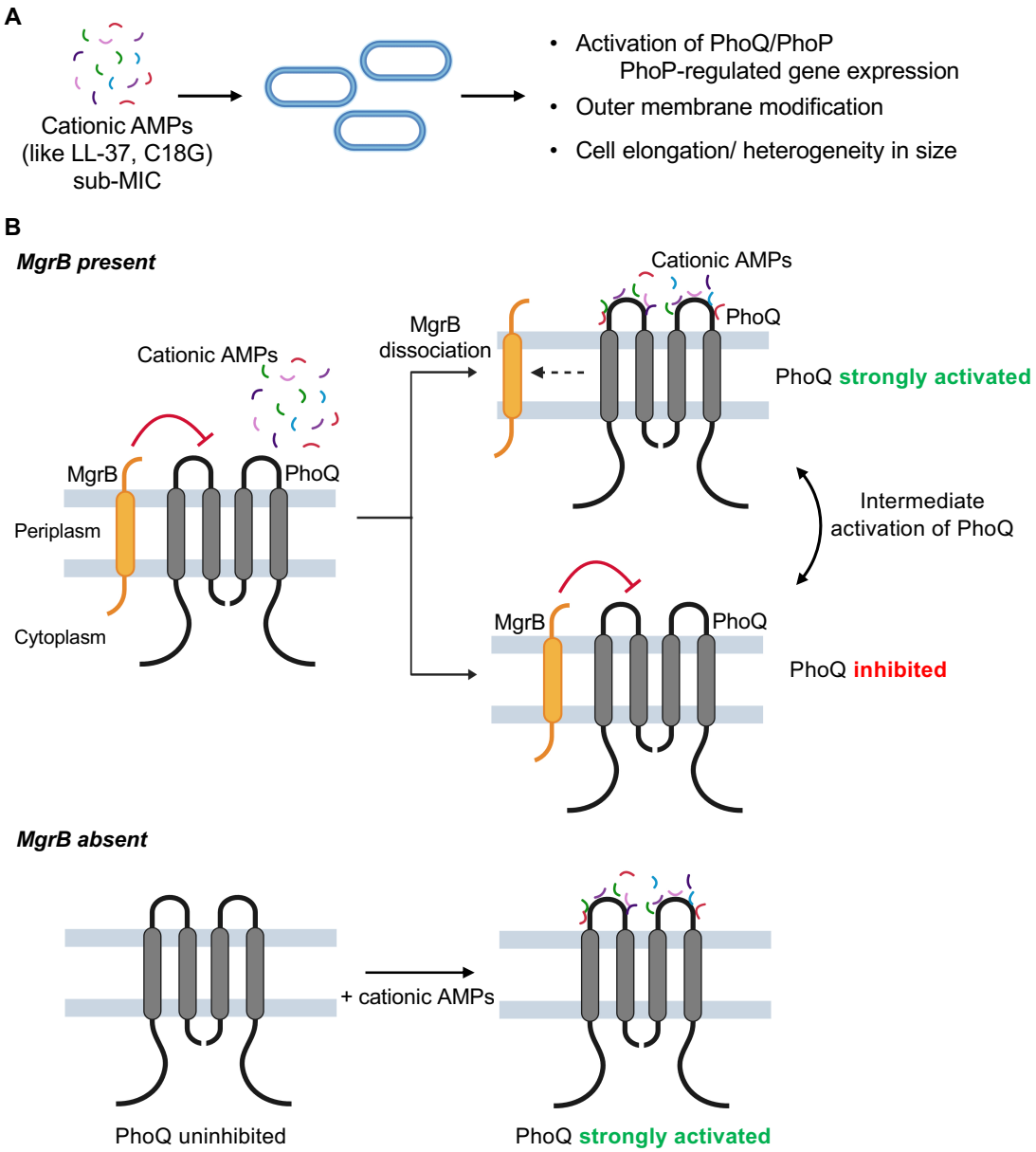
A
Cationic AMPs
(like LL-37, C18G)
sub-MIC
• Activation of PhoQ/PhoP
PhoP-regulated gene expression
• Outer membrane modification
• Cell elongation/ heterogeneity in size
B
MgrB present
Cationic AMPs
MgrB
PhoQ
Periplasm
Cytoplasm
MgrB
dissociation
Cationic AMPs
PhoQ
PhoQ strongly activated
Intermediate
activation of PhoQ
MgrB
PhoQ
PhoQ inhibited
MgrB absent
+ cationic AMPs
PhoQ uninhibited
PhoQ strongly activated

Supporting Information

Tables

Table S1. Minimum Inhibitory Concentration (MIC) and Minimum Bactericidal Concentration (MBC) values for LL-37 and its derivatives against *E. coli* strains. MIC values (μM) of antimicrobial peptide LL-37 and its derivatives KR-12 and RI-10 against different *E. coli* strains in supplemented minimal medium (Min A), Mueller Hinton broth (MHB), and tryptic soy broth (TSB). The corresponding MBC values (μM) are shown within parentheses. Data represent values obtained from three independent biological replicates.

***E. coli* strains**	**Media**	**LL-37**	**KR-12**	**RI-10**	**Gentamicin**
E.coli E423-17	Min A	2-4 (4)	8 (8)	>64 (>64)	2 (2)
	MHB	4-8 (8)	32 (32)	>64 (>64)	1 (1)
	TSB	4-8 (8)	32 (>32)	>64 (>64)	2 (4)
E.coli E416-17	Min A	4 (4)	4-8 (8)	>64 (>64)	2 (2)
	MHB	8 (8)	16 (16)	>64 (>64)	1 (2)
	TSB	8-16 (32)	16-32 (32)	>64 (>64)	4 (4)
E.coli 25922	Min A	2-4 (8)	1-2 (16)	>64 (>64)	2 (4)
	MHB	8 (8)	16 (32)	>64 (>64)	1 (2)
	TSB	8 (32)	32 (>32)	>64 (>64)	2-4 (4)

Table S2. List of peptides used in the study.

Peptide	Length	Amino acid sequence	Reference
LL-37	37	LLGDFFRKSKEKIGKEFKRIVQRIKDFLRNLVPRTES	(19)
KR-12	12	KRIVQRIKDFLR	(24)
RI-10	10	RIVQRIKDFL	(3)
KE-10	10	KEKIGKEFKR	(4)

Table S3. List of human LL-37 fragments that share the key recognition sequence for bacterial sensing (bolded).

Name	Peptide amino acid sequence
LL-37	LLGDFFRKSKEKIGKEF**KRIVQRIKDFLR**NLVPRTES
LL-23	LLGDFFRKSKEKIGKEFKRIVQR
LL-29	LLGDFFRKSKEKIGKEF**KRIVQRIKDFLR**
KR-20	**KRIVQRIKDFLR**NLVPRTES
KS-27	KSKEKIGKEF**KRIVQRIKDFLR**NLVPR
KS-30	KSKEKIGKEF**KRIVQRIKDFLR**NLVPRTES
RK-31	RKSKEKIGKEF**KRIVQRIKDFLR**NLVPRTES

Table S4. List of strains used in the study.

Strain	Relevant genotype	Reference/source
E. coli K12 MG1655	*λ⁻ rph-1*	*E. coli* Genetic Stock Center #7740
E. coli E423-17	Clinical antibiotic-resistant isolate	Wang lab, University of Nebraska Medical Center
E. coli E416-17	Clinical antibiotic-resistant isolate	Wang lab, University of Nebraska Medical Center
E. coli 25922	O6 isolate, reference strain for antibiotic susceptibility testing	ATCC
AML20	MG1655 *ΔmgrB* λ_{att} (P_{mgrB}-yfp) HK_{att} (P_{tetA}-*cfp*)	(5)
JNC21	MG1655 *ΔmgrB ΔqueE*::kan λ_{att} (P_{mgrB}-*yfp*) HK_{att} (P_{tetA}-*cfp*). kan^r	(6)
NRS6	MG1655 *ΔmgrB::kan ΔphoQ* λ_{att}::($P_{mgrBt7a}$-*yfp*) HK_{att}::(P_{tetA}-*cfp)*	This work
SAM31	MG1655 *ΔqueE* λ_{att} (P_{mgrB}-*yfp*) HK_{att} (P_{tetA}-*cfp*)	(6)
TIM92	MG1655 λ_{att} (P_{mgrB}-yfp) HK_{att} (P_{tetA}-*cfp*)	(7)
TIM100	MG1655 *ΔphoQ* λ_{att}::(P_{mgrB}-*yfp*) HK_{att}::(P_{tetA}-*cfp)*	(7)
TIM166	MG1655 *ΔphoQ* λ_{att}::($P_{mgrBt7a}$-*yfp*) HK_{att}::(P_{tetA}-*cfp)*	(7)

Figures

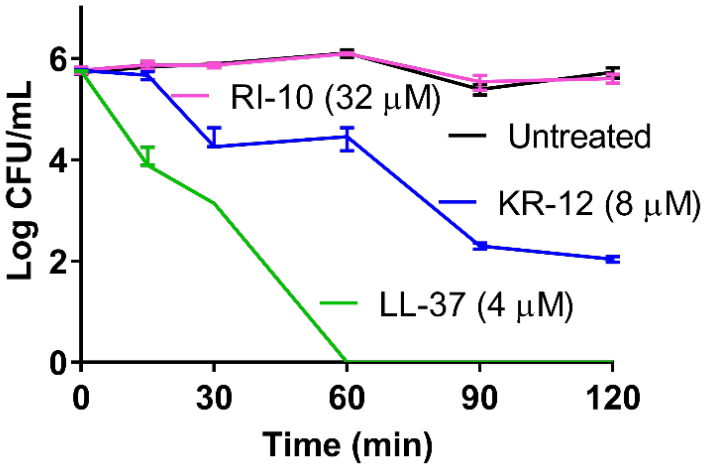

Figure S1. Killing kinetics LL-37, KR-12, and RI-10 against *E. coli* K-12 MG1655. Cells were treated with peptides at indicated concentrations in supplemented MinA with 0.1 mM $MgSO_4$. Data are represented as mean ± range for two biological replicates.

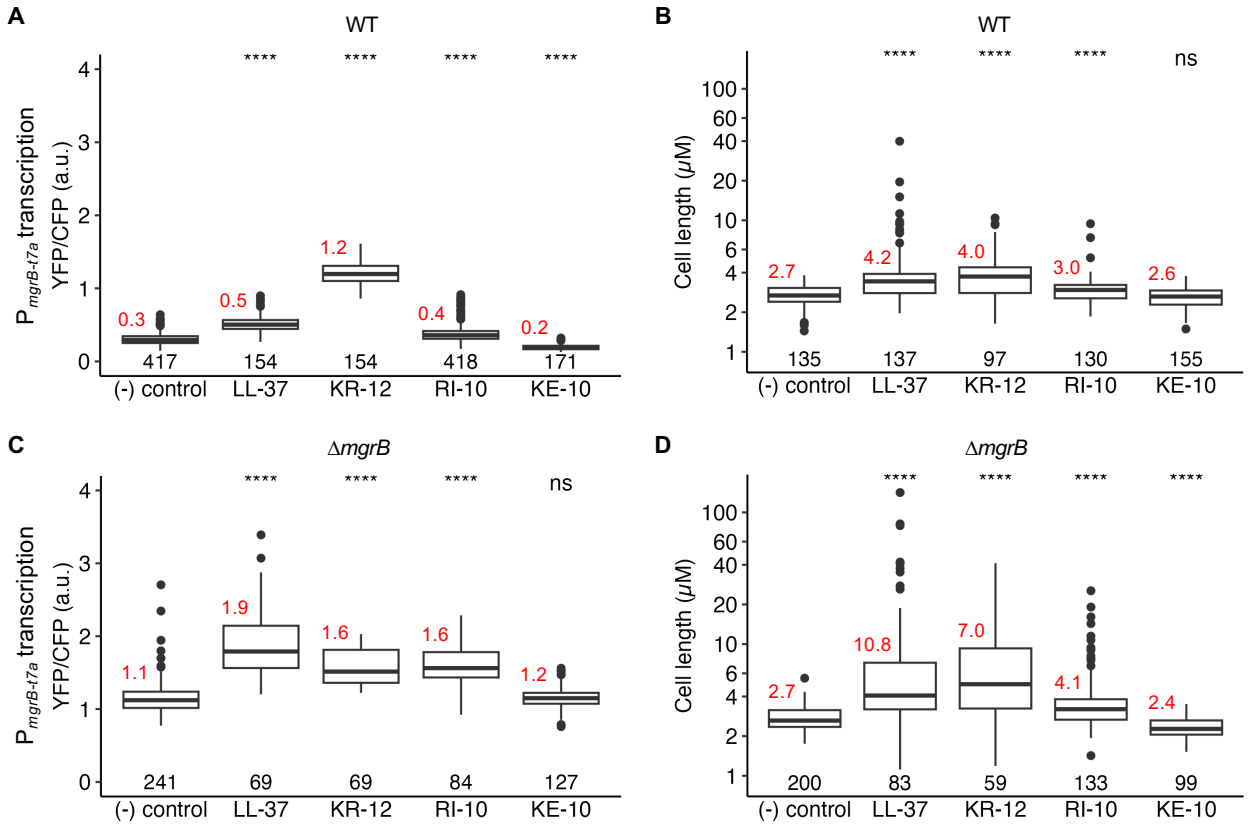

Figure S2. PhoQP-regulated transcription and cell lengths in *mgrB-t7a* reporter cells treated with sub-MIC levels of antimicrobial peptides. (A, C) PhoQP-dependent promoter reporter activity in wild-type (TIM166) or Δ*mgrB* (NRS6) cells, and **(B, D)** quantification of cell lengths of wild-type or Δ*mgrB* cells, grown in the presence of sub-MIC levels of the antimicrobial peptides LL-37 (1.25 μM), KR-12 (5 μM), RI-10 (5 μM), and KE-10 (5 μM) in supplemented MinA with 0.1 mM $MgSO_4$. Data are obtained from three biological replicates; mean and median values are shown in red text and black bars, respectively. The number of cells analyzed is indicated for each sample. P-values indicate the results of a Student's t-test: ****P ≤ 0.0001, ***P ≤ 0.001, **P ≤ 0.01, *P ≤ 0.05, and "ns" = P > 0.05.

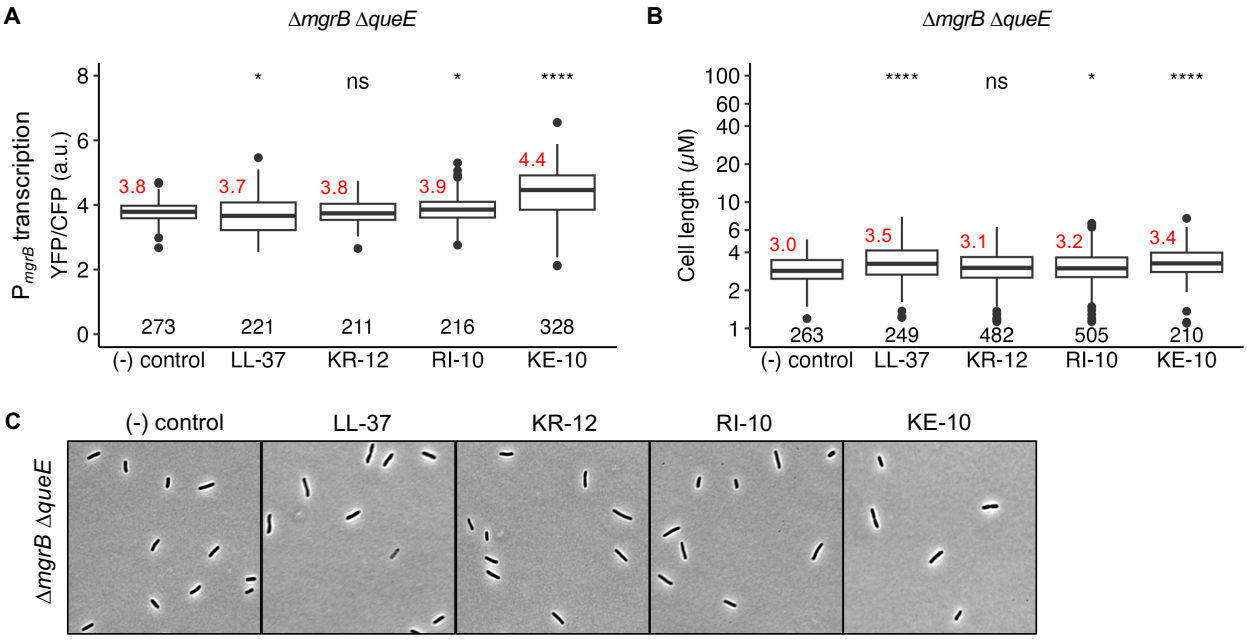

Figure S3. PhoQP-regulated transcription and cell lengths in Δ*mgrB* Δ*queE* cells treated with sub-MIC levels of antimicrobial peptides. (A) PhoQP-dependent promoter reporter activity, **(B)** quantification of cell lengths, and **(C)** phase contrast micrographs of Δ*mgrB* Δ*queE* (JNC21) cells grown in the presence of sub-MIC levels of the antimicrobial peptides LL-37 (1.25 μM), KR-12 (5 μM), RI-10 (5 μM), and KE-10 (5 μM) in supplemented MinA with 0.1 mM $MgSO_4$. Data are obtained from three biological replicates; mean and median values are shown in red text and black bars, respectively. The number of cells analyzed is indicated for each sample. P-values indicate the results of a Student's t-test: ****P ≤ 0.0001, ***P ≤ 0.001, **P ≤ 0.01, *P ≤ 0.05, and "ns" = P > 0.05.

References

1. J. Turner, Y. Cho, N. N. Dinh, A. J. Waring, R. I. Lehrer, Activities of LL-37, a cathelin-associated antimicrobial peptide of human neutrophils. *Antimicrob. Agents Chemother.* **42**, 2206–2214 (1998).

2. G. Wang, Structures of human host defense cathelicidin LL-37 and its smallest antimicrobial peptide KR-12 in lipid micelles. *J. Biol. Chem.* **283**, 32637–32643 (2008).

3. R. F. Epand, G. Wang, B. Berno, R. M. Epand, Lipid segregation explains selective toxicity of a series of fragments derived from the human cathelicidin LL-37. *Antimicrob. Agents Chemother.* **53**, 3705–3714 (2009).

4. A. F. Mechesso, Y. Su, J. Xie, G. Wang, Enhanced antimicrobial screening sensitivity enabled the identification of an ultrashort peptide KR-8 for engineering of LL-37mini to combat drug-resistant pathogens. *ACS Infect. Dis.* **9**, 2215–2225 (2023).

5. A. M. Lippa, M. Goulian, Feedback inhibition in the PhoQ/PhoP signaling system by a membrane peptide. *PLoS Genet.* **5**, e1000788 (2009).

6. S. S. Yadavalli, *et al.*, Antimicrobial peptides trigger a division block in Escherichia coli through stimulation of a signalling system. *Nat. Commun.* **7**, 12340 (2016).

7. T. Miyashiro, M. Goulian, Stimulus-dependent differential regulation in the Escherichia coli PhoQ PhoP system. *Proc. Natl. Acad. Sci. U. S. A.* **104**, 16305–16310 (2007).